BIOMAGNETIC LOCALIZATION FROM TRANSIENT QUASI-STATIC EVENTS

John C. Mosher, Richard M. Leahy, and Paul S. Lewis

Los Alamos National Laboratory, MEE-3, Los Alamos, NM 87545
Signal and Image Processing Institute, University of Southern California, Los Angeles, CA 90089-2564

ABSTRACT

Sensory stimuli, such as auditory, visual, or somatosensory, evoke neural responses in very localized regions of the brain. A SQUID biomagnetometer can measure the very weak fields that are generated outside of the head by this response. A simple source and head model of current dipoles inside a conducting sphere is typically used to interpret these magnetic field measurements or magnetoencephalogram (MEG). Locating dipole sources using data recorded from an array of biomagnetic sensors is distinguished from conventional array source localization techniques by the quasi-static transient nature of the data. Here, the basic MEG model is reviewed, then a localization example is given to motivate the need for partitioning the data to improve estimator performance. Time-eigenspectrum analysis is introduced as a means of partitioning and interpreting spatio-temporal biomagnetic data. Examples using both simulated and somatosensory data are presented.

1. INTRODUCTION

A sensory stimulus, such as auditory, visual, or somatosensory, evokes a neural response in a very localized region of the brain. An array of Superconducting QUantum Interference Device (SQUID) biomagnetometers may be used to measure the very weak magnetic field generated by these neural currents. These magnetic field measurements or magnetoencephalogram (MEG) provide a non-invasive method for studying functional activity in the human brain with millisecond temporal resolution. One approach to the interpretation of MEG data is to estimate the parameters describing the internal sources that produce the evoked field.

The inverse problem in MEG is highly ill-posed unless a simplifying source model is introduced. The simplest model for an evoked response is the "dipole in a sphere," where the primary neural currents are modeled as a current dipole or set of dipoles, and the head is modeled as a set of homogeneous spherical conductive shells. The global volume currents distributed over the shells are modeled as the return currents from these dipoles. The model for MEG contains a transfer function or lead field model that relates the dipoles' intensities, orientations, and locations to the externally measured field. The general inverse problem is then to find the location and moment parameters that describe each dipole.

The simplest approach to localization is to fit one or more dipoles to each temporal snapshot. Our previous study of the Cramer-Rao Lower Bounds (CRLB) [2] associated with MEG based localization of multiple dipoles indicates that acceptable accuracy will probably not be attained with a single snapshot. Under the assumption that the dipole is "stationary," i.e., the sources do not move over time, multiple snapshots can be used to improve localization accuracy [3].

An important property of evoked response measurements is that they are inherently transient. The transient evoked response is typically captured inside a larger acquisition window, and no generally agreeable temporal model exists to assist in isolating the response from the background activity and experimental artifacts. In this paper, we introduce a technique for parsing the data to isolate the transient events using the SVD of the spatio-temporal data as a function of window width and delay. In addition, this technique can be used to identify the total number of dipoles involved and their individual activation periods within the transient event.

2. FORWARD MODEL

The simplest model in use is a dipole in a spherically symmetric head. Radially oriented dipoles produce no magnetic field outside the concentric conducting spheres, regardless of the number of spheres we consider, and return volume currents produce no external magnetic fields in the radial direction. Sarvas [4] provides a thorough derivation of the general MEG formulas, then presents the simplifications that result for the spherically symmetric head model with radially oriented sensors. For radially oriented sensors, the measured field is a relatively simple function of only the tangential components of the dipole moments. The radially oriented MEG sensor coil is assumed to make a point measurement of the radial magnetic field. For a dipole located at l, the scalar radial magnetic field $B(p)$ at sensor location p can be expressed as the inner product of gain vector g and the dipole moment q,

$$B(p) = g^T(l, p)\, q \ . \qquad (EQ\ 1)$$

This work was supported by the Los Alamos National Laboratory, operated by the University of California for the United States Department of Energy under contract W-7405-ENG-36, and by the Kaprielian Innovative Research Fund at the University of Southern California. Correspondence to: Dr. R. Leahy, Signal & Image Processing Institute, University of Southern California, Los Angeles, CA 90089-2564.

0-7803-0946-4/93 $3.00

For the case of the spherical head model and the radial sensor measurements, this gain vector is a special case of the Biot-Savart law and can be expressed as

$$g^T(l,p) = \left(\frac{\mu_0}{4\pi}\right)\frac{r \times l}{\|p-l\|^3} \qquad (EQ\ 2)$$

where the coordinate system is assumed to be head centered, r is the unit radial orientation of the sensor coil, μ_0 is the permeability of free space, and " $\times$ " denotes the vector cross product.

For multiple dipoles, the vector of measured samples at time t can be modeled as

$$A(t) = \left[G(l_1)\ G(l_2)\ \ldots\ G(l_p)\right]\begin{bmatrix} q_1(t) \\ q_2(t) \\ \ldots \\ q_p(t) \end{bmatrix}$$

$$= G(l)\,q(t) \qquad (EQ\ 3)$$

where $A(t)$ represents the column vector of magnetic field measurements. The vector l_i represents the three-dimensional location of the ith current dipole, and $q_i(t)$ represents the corresponding three-dimensional dipole moment at time t. The MEG gain matrix $G(l_i)$ for a single dipole is the concatenation of all gain vectors $g(l_i)$ for all sensor locations. $G(l_i)$ represents the "gain transfer" matrix for the ith dipole, which relates the dipoles' moments to the vector of measurements and has a nonlinear dependence on the dipole locations. Column vectors l and $q(t)$ are both concatenations of the parameters for p dipoles,

$$l = \left[l_1, \ldots, l_p\right]^T \text{ and } q(t) = \left[q_1(t), \ldots, q_p(t)\right]^T.$$

3. LOCALIZATION

An important inverse problem is to determine the location of the dipoles that could generate the observed spatio-temporal data. In [1], we examined localization based on standard nonlinear least-squares and showed that the various models could be brought into a unifying algebraic model to which modern array processing techniques could be applied. Problems associated with the nonlinear least-squares method include strong local minima and unknown model order. By introducing a variation of "diversely polarized" MUSIC, we were able to scan the three dimensional volume of the brain searching for multiple dipoles and thus avoid local minima. The number of elemental dipole sources is determined by the rank of the signal subspace.

Least-squares and subspace estimators implicitly or explicitly make use of the spatial correlation matrix. In a typical MEG application, we might collect 200 ms of data, yet observe that the signal only exists from about 75 ms to 125 ms. If we form the spatial correlation matrix from the entire 200 ms of data, we reduce the SNR in the correlation matrix by effectively averaging in too much noise, which degrades estimator performance.

As an example, we simulated a spherical head model and 37 sensor array pattern, as described in [2]. We simulated the placement of two dipoles spaced two cm apart just under the surface of the skull, and gave each dipole a Hamming window shaped activation sequence with a peak amplitude of 10 nanoamps. The sequences were arranged such that the first dipole fired completely, then the second dipole fired with no overlap with the first. The overlay of all simulated time series measured at the 37 sensors is shown in the top portion of Fig. 1.

A nonlinear least squares estimator (as described in [1]) was then run with 200 different realizations of white random noise with a standard deviation of 70 femtoteslas. The choice of signal strength and noise selections are described in [2]. The standard deviations on the localization error for the two dipoles was 1.81 mm and 2.14 mm, when estimated using all of the data.

We then partitioned the sequence in half, reducing the estimation to two one-dipole problems. The standard deviation on the localization error drops to 1.00 mm and 1.13 mm for the two dipoles. Thus the partitioning of the data from one two-dipole problem into two one-dipole problems improved the efficiency of the estimator.

This simulation assumed known model order. By focusing the problem to two one-dipole problems, the nonlinear estimator can discard noisy snapshots that degrade its performance. As discussed in [1], MEG-MUSIC was introduced to overcome some of the problems with order selection and local minima encountered in nonlinear least-squares. However, estimating the subspace also requires careful attention to partioning, since the subspace estimates are sensitive to noisy snapshots.

In order to improve the subspace and localization estimates, we must identify the extents of the events of interest and partition the time series accordingly. Most signal detection algorithms rely on an explicit temporal model, but temporal models in MEG research are subject to controversy. Consequently, a nonparametric approach to partitioning is more appropriate.

4. TIME-EIGENSPECTRUM ANALYSIS

We approach the partitioning problem by using the temporal coherence across the sensors evident from the quasi-static formulation of the problem. Time-eigenspectrum (TE) analysis is a novel method of examining the similarity of the response of several sensors over a prescribed block of time. As the intensity of a dipolar source fluctuates, its signal arrives simultaneously at all sensors. If we place an appropriately sized window at the proper instance in time around a single dipole, we find that the rank of this window is one, i.e., the temporal signals arriving at all sensors are perfectly coherent. If two independent signals are active in this window, we observe that the rank is two.

At a particular instance in time, we begin the analysis by creating a window of width one. Obviously, a single time slice is perfectly similar with itself. We proceed by adding the previous time slice to form a window of width two, then three, four, etc., until we reach some upper window width by design or data limitation. For each window width, we take a measure of the similarity of the window, described below. We then slide this window forward one time slice,

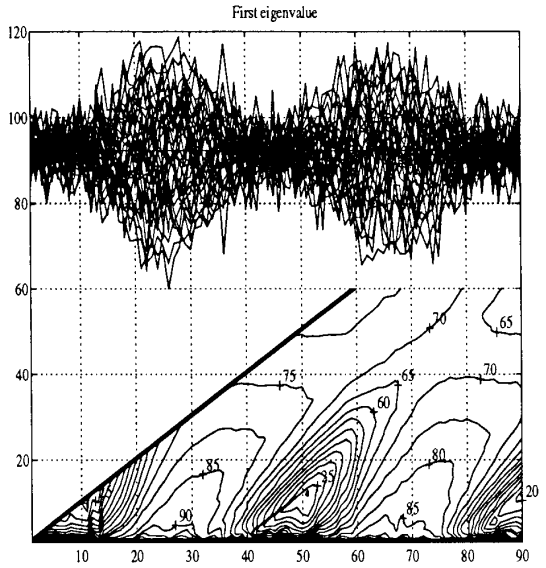

FIGURE 1. Simulation Time-Eigenspectrum. The rank 1 contour plots reveal that the two signals together are insufficiently described by a rank one subspace. Each signal can however be temporally isolated.

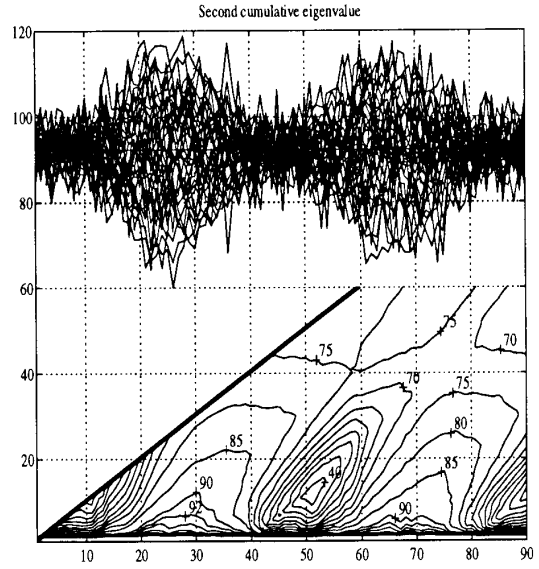

FIGURE 2. Simulation Time-Eigenspectrum (cont'd). The rank 2 contour plots reveal that the individual responses are not much improved with a second eigenvalue.

and repeat the process. The result is a two-dimensional function, $f(t,w)$, with one dimension corresponding to the most recent sample, t, in the window and the other the window width, w.

The similarity measure we employ is multidimensional and is derived from the singular values obtained from an SVD of the window. We form a matrix from w sequential snapshots of the data, ending at time slice $\mathbf{A}(t)$. Denoting the singular values by the ordered vector $s(t,w)$, we form a vector of the cumulative square of the singular values, normalized by the sum of the squared singular values. Thus, the jth element of the vector similarity measure at time t for window width w is calculated as

$$s(t, w) = \text{svd}([\mathbf{A}(t-w+1)\ldots\mathbf{A}(t)])$$

$$f_j(t, w) = \frac{\sum_{i=1}^{j} s_i^2(t, w)}{\| s(t, w) \|^2} \qquad (EQ\ 4)$$

for $j = 1,\ldots,$ min(w,m), where m is the number of sensors.

The element of our measure vector that approaches unity is our indication of the rank of the window; the last element of f is always unity. Thus a rank two window would have its second and greater elements equal to 1. In practice, noise always prevents such a perfect rank estimate, but this SVD-based measure f allows us to observe at which element we are "close enough" to a lower rank matrix.

4.1. Simulation

Using the Hamming-shaped activation sequence described above, we simulated two dipoles firing sequentially. The noiseless time series was five points of no signal, then a 40 point Hamming sequence for the first dipole, then a 40 point Hamming sequence for the second, then finally 5 points of no signal, for a total of 90 samples. The time trace across all 37 simulated sensors is shown in the top portions of Fig. 1 and Fig. 2, with additive random white noise; the standard deviation was 70 femtoteslas. The bottom portions of these figures show the rank 1 and rank 2 time-eigenanalysis contours, i.e., $f_1(t,w)$ and $f_2(t,w)$ respectively. The abscissa gives the time index of the leading edge of the window, and the ordinate gives the width of the sliding window.

The contour intervals indicate the percentage of total "energy" (square of the Frobenius norm) in the window contained in the subspace. In Fig. 1, the contours are above 80% for small windows centered on the responses, indicating that 80% of the signal energy in the given window can be described by the first eigenvalue. The contours rapidly drop for small windows centered on the noise intervals, and the contour shows that the first eigenvalue only accounts for 25% of the signal energy in the transistion and end regions. Although the center of the responses is visible in this simulated data, the transistions in the contours more clearly show the segments dominated by either noise or signal.

In Fig. 2, the contours represent the percentage energy contained by the first two dipoles. The windows containing only one active dipole show small increases in percentage energy that those containing both dipoles. The 75% contours are beginning to merge in the upper regions which rep-

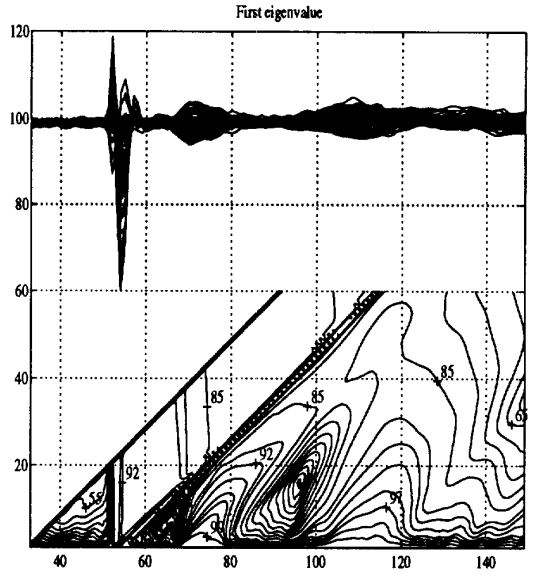

FIGURE 3. Ring Finger Stimulation, Rank 1 analysis.

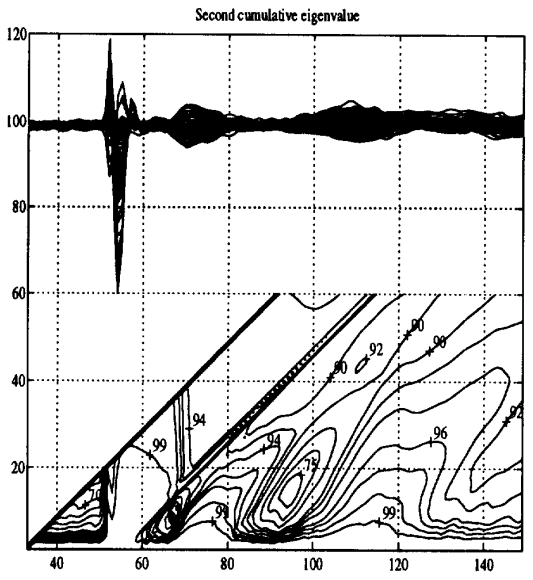

FIGURE 4. Ring Finger Stimulation, Rank 2 analysis.

resent windows that encompass both dipoles. Although the noiseless data is rank two, the proximity of the dipoles and the intensity of the noise make it difficult in this simulation to distinguish the overall data as rank two; however, we do appear clearly justified in partitioning the data into two distinct sets.

This simulation is somewhat transparent, since the two response sequences are mostly visible, and prudent partitioning might be possible by inspection alone. However, the simulation was simplified to highlight some of the contours seen in actual data and to assist in their interpretation. In the next example, we apply this technique to MEG somatosensory data.

4.2. Somatosensory Response

In this experiment, biomagnetic sensors at 77 positions about the surface of the head recorded the evoked response of the ring finger to piezoelectric stimulation. Fig. 3 and Fig. 4 show in their top portions the overlay of the response (averaged from 300 trials) across all sensors. The time index corresponds to 2 ms intervals, and the first 20 samples visible are part of the pre-stimulus interval. A stimulus artifact is present at time sample 55, and the first dominant neural response occurs 40 ms later at time index 75. A secondary response is evident beginning around time sample 100.

We ignore the stimulus artifact and focus on the two evoked responses. The contours indicate that the first response is of low rank for only about 15 samples and is preceded and followed by relatively incoherent and low power regions. The second response appears to lie more appropriately in a rank 2 subspace, but only up to about time sample 125. Although the signal levels remain relatively active beyond sample 125, the contours indicate a drop in similarity.

The contour transitions guide how we might partition the data to extract the two responses. The first response region is also obvious in the data, but not so obvious is the high rank of the low power regions surrounding it. The onset of the second response is also somewhat visible in the data, but the contours assist in trimming the upper end of the response, where visible inspection of the data does not indicate where we should trim.

Finally, we comment on the computational load in performing the numerous SVDs required. The two examples presented each required about five minutes on a SPARC 330 or fifteen minutes on a 486-33 MHz, both running MATLAB.

References

[1] J.C. Mosher, P.S. Lewis, and R.M. Leahy, "Multiple dipole modeling and localization from spatio-temporal MEG data," *IEEE Trans. Biomedical Eng*, 1992, 39:541-557.

[2] J.C. Mosher, M.E. Spencer, R.M. Leahy, and P.S. Lewis, "Error bounds for EEG and MEG dipole source localization," *Electroencephalography and clinical Neurophysiology* (in press) 1993.

[3] M. Scherg and D. von Cramon, "Two bilateral sources of the late AEP as identified by a spatio-temporal dipole model," *Electroencephalography and clinical Neurophysiology*, vol 62, pp. 32—44, 1985.

[4] J. Sarvas, "Basic mathematical and electromagnetic concepts of the biomagnetic inverse problem," *Phys. Med. Biol.*, 1987, 32:11-22.